

ESTIMATION AND FORECASTING OF IONOSPHERIC TOTAL  
ELECTRON CONTENT BASED ON NEURAL NETWORK AND  
HYBRID SEASONAL AUTOREGRESSIVE INTEGRATED  
MOVING AVERAGE-NEURAL NETWORK MODELS OVER  
EQUATORIAL REGION

VIKNESWARY JAYAPAL

UNIVERSITI SAINS ISLAM MALAYSIA  
جامعة العلوم الإسلامية  
ISLAMIC SCIENCE UNIVERSITY OF MALAYSIA

UNIVERSITI SAINS ISLAM MALAYSIA

ESTIMATION AND FORECASTING OF IONOSPHERIC TOTAL  
ELECTRON CONTENT BASED ON NEURAL NETWORK AND  
HYBRID SEASONAL AUTOREGRESSIVE INTEGRATED  
MOVING AVERAGE-NEURAL NETWORK MODELS OVER  
EQUATORIAL REGION

Vikneswary Jayapal  
(Matric No. 4130261)

Thesis submitted in fulfillment for the degree of  
DOCTOR OF PHILOSOPHY  
SCIENCE AND TECHNOLOGY

Faculty of Science and Technology  
UNIVERSITI SAINS ISLAM MALAYSIA  
Nilai

July 2016

## DECLARATION OF THESIS AND COPYRIGHT

### إقرار البحث العلمي وحق النشر

Student's Full Name / اسم الطالب بالكامل	VIKNESWARY JAYAPAL		
Academic Session / الفصل الدراسي	2013/2014	Matric No. / رقم التسجيل الجامعي	4130261
Research Title / عنوان البحث	ESTIMATION AND FORECASTING OF IONOSPHERIC TOTAL ELECTRON CONTENT BASED ON NEURAL NETWORK AND HYBRID SEASONAL AUTOREGRESSIVE INTEGRATED MOVING AVERAGE - NEURAL NETWORK MODELS OVER EQUATORIAL REGION		

I hereby declare that the work in this thesis/ project paper is my own except for quotations and summaries which have been duly acknowledged /

إني أقر وأعترف بأن هذا البحث من عملي وجهدي الشخصي، أما مقتطفات والاقباسات، فقد أشرت إلى مصادرها في هامش البحث

I acknowledged that Universiti Sains Islam Malaysia reserves the right as follows /

أقر بأن تحتفظ جامعة العلوم الإسلامية الماليزية بالحقوك التالية:

1. The thesis/ postgraduate project paper is the property of Universiti Sains Islam Malaysia / إن ملكية هذا البحث العلمي لجامعة العلوم الإسلامية الماليزية
2. The library of Universiti Sains Islam Malaysia has the right to publish my thesis/ postgraduate project paper as online open access (fulltext) and make copies for the purpose of research or teaching and learning only /

تحتفظ مكتبة جامعة العلوم الإسلامية الماليزية بحق النشر لهذا البحث العلمي أو المشروع العلمي على الإنترنت (البحث الكامل) وحق الطباعة بهدف إجراء البحث العلمي أو التعليم والتعلم فقط

.....  
(Student's Signature)

.....  
(Supervisor's Signature)

820523-08-5060

.....  
(IC No./Passport No.)

.....  
(Name)

.....  
(Date)

.....  
(Date)

## BIODATA OF AUTHOR

**Vikneswary Jayapal** (4130261) was born in Perak, Malaysia on 23<sup>rd</sup> May 1982. She is currently residing at Batu Gajah, Perak.

Vikneswary received her B. Eng. (Hons) degree in Electrical (Telecommunications) Engineering from Universiti Tun Hussein Onn Malaysia, in 2006. Upon completion her first degree, she was attached with Agilent Technologies, Penang Malaysia, in 2006 as a RF engineer. In 2007, she joined the Department of Communication Engineering, Universiti Tun Hussein Onn Malaysia as a tutor. She then took a leave of absence to pursue her studies and obtained her M.Eng degree in Electrical, Electronics and Telecommunications from Universiti Teknologi Malaysia, in 2009. Her master's project was on security in Wireless Sensor Network using IPV6.

At present, she is a Ph.D. candidate at Faculty of Science and Technology, Universiti Sains Islam Malaysia. Her current research interests are in modelling the Earth's ionosphere, radio propagation in the equatorial ionosphere, linear and non-linear estimation models.



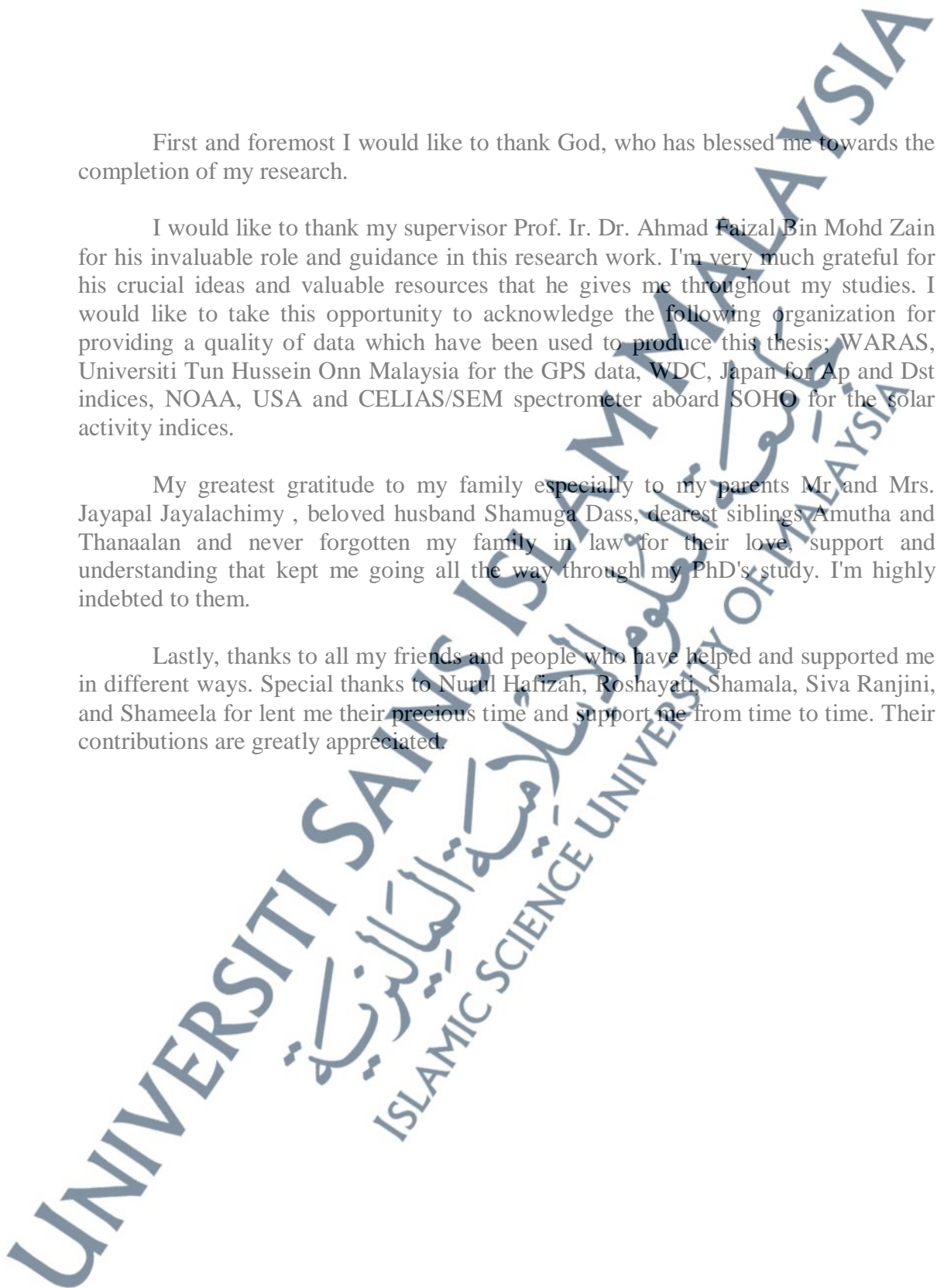
## ACKNOWLEDGEMENTS

First and foremost I would like to thank God, who has blessed me towards the completion of my research.

I would like to thank my supervisor Prof. Ir. Dr. Ahmad Faizal Bin Mohd Zain for his invaluable role and guidance in this research work. I'm very much grateful for his crucial ideas and valuable resources that he gives me throughout my studies. I would like to take this opportunity to acknowledge the following organization for providing a quality of data which have been used to produce this thesis; WARAS, Universiti Tun Hussein Onn Malaysia for the GPS data, WDC, Japan for Ap and Dst indices, NOAA, USA and CELIAS/SEM spectrometer aboard SOHO for the solar activity indices.

My greatest gratitude to my family especially to my parents Mr and Mrs. Jayapal Jayalachimy , beloved husband Shamuga Dass, dearest siblings Amutha and Thanaalan and never forgotten my family in law for their love, support and understanding that kept me going all the way through my PhD's study. I'm highly indebted to them.

Lastly, thanks to all my friends and people who have helped and supported me in different ways. Special thanks to Nurul Hafizah, Roshayati, Shamala, Siva Ranjini, and Shameela for lent me their precious time and support me from time to time. Their contributions are greatly appreciated.



## ABSTRAK

Kebolehubahan jumlah kandungan elektron (TEC) yang tidak dapat diramal di kawasan khatulistiwa dan kekosongan dalam pengkalan data TEC yang disebabkan oleh kegagalan infrastruktur Bumi mewujudkan keperluan untuk membangunkan satu teknik penganggaran TEC. Pendekatan berasaskan NN didapati sangat sesuai di dalam pemodelan parameter ionosfera kerana keupayaannya yang fleksibel memeta fungsi tak linear, yang boleh menganggarkan sebarang fungsi boleh ukur tak linear dengan ketepatan yang dikehendaki. Kajian ini mengemukakan pembangunan model rangkaian neural (NN) untuk menganggar TEC ionosfera bagi sebuah stesen penerima GPS tunggal (Lat.  $1^{\circ}52'N$ , Long.  $103^{\circ}48'E$ , Junaman magnetik  $14.3^{\circ}$ ) di Malaysia dari Februari 2005 hingga Desember 2006. Di dalam NN, kebolehubahan TEC dimodelkan sebagai fungsi untuk variasi harian, variasi bermusim, solar, dan proksi magnet. Model NN1 dan NN2 masing-masing digunakan untuk menginterpolasi (tentu dalam) dan mengekstrapolasi (tentu luar) data TEC setiap jam yang hilang. Keupayaan NN menginterpolasi boleh dilihat dengan lebih jelas berbanding dengan mengekstrapolasi, terutamanya bagi tempoh yang lebih panjang untuk data yang hilang. Model NN2 mengalami lebih banyak kesukaran dalam mengekstrapolasi (tentu luar) nilai TEC pada waktu malam berbanding waktu siang. Model NN2 mempunyai pembetulan relatif (Crel) kurang daripada 85% apabila data TEC yang hilang adalah lebih daripada 60%. Bagi pengesahsahihan model, nilai TEC bagi NN2 dibandingkan dengan model Ionosfera Rujukan Antarabangsa (IRI) berdasarkan kepada GPS TEC. Keputusan anggaran bagi empat musim pada tahun 2006 menunjukkan bahawa, model NN2 sepadan dengan GPS TEC ketika musim solstis. Dari segi purata RMSE, model NN2 menunjukkan peningkatan sebanyak 39.9% berbanding dengan model IRI bagi empat musim tersebut. Kebolehamalan TEC semasa peristiwa spontan menunjukkan bahawa model IRI-2007 cenderung untuk memberikan hasil anggaran yang lebih tepat berbanding dengan model NN2 semasa ribut ionosfera negatif dengan Crel kira-kira ~25% lebih tinggi daripada model NN2. Sebaliknya, model NN2 mampu menjanakan trend TEC yang lebih baik berbanding dengan model IRI semasa kesan ribut ionosfera positif dengan Crel kira-kira ~30 hingga 35% lebih tinggi daripada model IRI. Selain penganggaran, model ramalan TEC ionosfera juga sangat bermanfaat sebagai sistem amaran awal bagi mengurangkan kesan cuaca buruk di angkasa dan bencana alam terhadap kehidupan manusia dan teknologi. Berdasarkan data pembaikan GPS TEC, model ramalan siri masa dibangunkan dengan menggunakan model hybrid yang mengintegrasikan purata gerakan bersepadu autoregresif bermusim (SARIMA) dan rangkaian neural untuk meramal nilai TEC sehingga tiga hari lebih awal. Nilai ramalan TEC daripada model hybrid dibandingkan dengan model individu SARIMA (FCAST-SARIMA) dan NN (FCAST-NN) secara berasingan berdasarkan kepada GPS TEC. Keputusan menunjukkan bahawa nilai TEC bagi ketiga-tiga model ramalan agak baik semasa keadaan tenang. Sementara itu, pencapaian model individu turun semasa keadaan sederhana, dan ralat ramalan meningkat pada kedua-dua model tunggal apabila ufuk masa menjadi lebih besar. Selain itu, dari segi purata RMSE, peningkatan peratusan model hybrid terhadap SARIMA dan NN semasa keadaan terganggu ialah masing-masing mencatatkan ~13.4% dan ~26.1%. Model penganggaran (*estimation*) dan peramalan (*forecasting*) digunakan secara bersama-sama untuk menyediakan satu kajian yang menyeluruh mengenai pemodelan ionosfera TEC di Parit Raja, Malaysia.

## ABSTRACT

Unpredictable variability of total electron content (TEC) in the equatorial region and gaps in the TEC database due to Earth infrastructure failures creates a need to develop a TEC estimation model. NN-based approaches are found promising in modelling the ionospheric parameters because they have flexible non-linear function mapping capability, which can estimate any non-linear measurable function with arbitrarily desired accuracy. This work presents, the development of neural network (NN) based model to estimate the ionospheric TEC for a single GPS receiver station (Lat.  $1^{\circ}52'N$ , Long.  $103^{\circ}48'E$ , Magnetic dip  $14.3^{\circ}$ ) over Malaysia from February 2005 to December 2006. In NN, the TEC variability is modelled as a function of diurnal variation, seasonal variation, solar and magnetic proxies. The NN1 and NN2 models are used to interpolate and extrapolate the missing hourly TEC data, respectively. The NN's interpolation capability could be seen more evidently than the extrapolation, especially over longer periods of missing data. The NN2 model experienced difficulty in extrapolating the TEC values during the night time than the daytime. The NN2 has relative correction (Crel) below than 85% when the missing TEC data are above 60%. For model validation, TEC values from NN2 are compared with the International Reference Ionosphere (IRI) model with respect to GPS TEC. The estimation results for the four seasons in 2006 show that, the NN2 model agrees well with GPS TEC during solstice seasons. In terms of average root mean square error (RMSE), NN2 model shows an improvement about 39.9% compared to the IRI model over the four seasons. The predictability of TEC during negative ionospheric storm revealed that the IRI-2007 model tends to yield more accurate estimation results than the NN2 model with Crel is about ~25% higher than NN2 model. Conversely, the NN2 model able to generalize the TEC trend more favourably than the IRI model during positive ionospheric storm effects with Crel is about ~30 to 35% higher than the IRI model. Besides estimation, an ionospheric TEC forecasting model can be highly beneficial as an early warning system in order to lessen the adverse space weather and natural hazard impacts on human life and technologies. Based on the recovery GPS TEC data, a time series forecasting model is developed using a hybrid model that integrates the seasonal autoregressive integrated moving average (SARIMA) and neural networks to forecast the TEC values up to three days ahead. The forecast TEC values from the hybrid model are compared with the individual models SARIMA (FCAST-SARIMA) and NN (FCAST-NN) separately with respect to GPS TEC. Results show that all the three models forecast TEC values fairly well during quiet condition. Meanwhile, the performance of the individual models degraded during moderate condition and the forecasting errors increased for both the single models as the time horizon became larger. Besides, in term of average RMSE the percentage improvements of the hybrid model over SARIMA and NN during disturbed condition are ~13.4% and ~26.1%, respectively. The estimation and forecasting models are used in tandem to provide a complete investigation on ionospheric TEC modelling at Parit Raja, Malaysia.

## ملخص الأطروحة

نموذج التنبؤ بالمحتوى الكامل للألكترونات في غلاف الأيونوسفير يمكن أن يكون ذا جدوى عالية، حيث يستخدم لأنظمة التحذير المبكر والذي يساعد في التقليل من تأثير الفضاء العكسي على حياة الإنسان والتقنية. عدم صحة البيانات وفقدتها يمكن أن يؤثر سلباً على أداء نموذج التنبؤ. هذه الأطروحة تتحقق من قدرة تقنية الشبكات العصبية في التنبؤ بالمحتوى الكامل للألكترونات لمحطة استقبال اشارة نظام تحديد المواقع GPS والتي تقع على خط عرض ٥٢°١ شرقاً وبخط طول ٤٨°١٠٣ غرباً وثنائي قطبية مغناطيسية ١٤,٣° لتوليد بيانات ملائمة المحتوى الكامل للألكترونات في ماليزيا. في تقنية الشبكات العصبية، تغير المحتوى الكامل للألكترونات تمت نمذجته كدالة في التغير اليومي والتغير الفصلي و أيضاً كدالة في المفوض الشمسي و المغناطيسي. ولزيادة التحقق، الشبكة العصبية لقيم المحتوى الكامل للألكترونات قد تمت مقارنتها مع المحتوى الكامل للألكترونات لأشارة نظام تحديد المواقع وكذلك مع النموذج العالمي IRI TEC. نموذج الشبكات العصبية يستخدم لأستيفاء و استقراء البيانات الضائعة المحتوى الكامل للألكترونات للنظام العالمي لتحديد المواقع. قدرة استيفاء نموذج الشبكات العصبية يمكن رؤيته بوضوح بالمقارنة مع قدرة الإستقراء خصوصاً للفترات الطويلة من البيانات الضائعة.

نموذج الشبكات العصبية يواجه صعوبة اكبر في استقراء قيم المحتوى الكامل للألكترونات خلال الأوقات الليلية أكثر من أي وقت آخر، حيث لديه دقة أقل من ٨٥٪ عندما تكون قيم معدل ضياع البيانات اكبر من ٦٠٪. علاوة على ذلك، نتائج التنبؤ لفصول السنة الأربعة لسنة ٢٠٠٦ تبين أن نموذج الشبكات العصبية يميل لتنبؤ قيم المحتوى الكامل للألكترونات بشكل أكثر اعتدالاً مقارنة مع النموذج العالمي IRI-2007. نموذج الشبكات العصبية متلائم جداً مع المحتوى الكامل للألكترونات الخاص بنظام تحديد المواقع العالمي خلال فصول انقلاب الشمس أكثر من ما هو خلال فصول تساوي الليل مع النهار. من ناحية متوسط RMSE نموذج الخلايا البصرية تبين تحسن بمقدار ٢٩,٩٪ مقارنة بالنموذج العالمي IRI-2007. امكانية تطبيق نموذج الشبكات البصرية للتنبؤ بمحتوى الألكترونات الكامل الغير مرئي لغلاف الأيونوسفير خلال الأحداث المتهورة قد تمت دراستها. نموذج RII-2007 في العموم يميل لأعطاء تنبؤات للنتائج بأكثر دقة مقارنة بنموذج الشبكات العصبية خلال العواصف السالبة للأيونوسفير مع دقة تساوي تقريباً ٢٥٪ اكثر بالمقارنة بنموذج الشبكات البصرية. لكن نموذج الشبكات البصرية قادر على استقراء اتجاه المحتوى الكامل للألكترونات بشكل أفضل من نموذج IRI خلال ظواهر عواصف الأيونوسفير الموجبة أعلى بحوالي ٣٠ الى ٣٥٪. هذا العمل قد تم توسعته بإستخدام استرداد المحتوى الكامل للألكترونات لأنظمة تحديد المواقع حيث تم تطوير نموذج التنبؤ بإستخدام نموذج مهجن والذي يجمع كلاً من: الشبكات العصبية و معدل الإنحدال المتحرك المتكامل الفصلي (SARIMA). النموذج يستخدم لتوليد المحتوى الكامل للألكترونات لطبقة الأيونوسفير لمدة تصل الى ثلاثة أيام مستقبلية و مقارنتها مع القيم الفعلية وكذلك قيم التنبؤ لنماذج SARIMA و نموذج الشبكات البصرية بشكل منفصل. النتائج توضح أن كلا النموذجين تعطي أداء يمكن مقارنته مع النموذج الهجين خلال وضع السكون. في الوقت ذاته، أداء كلا النموذجين يتضعع خلال الوضع المعتدل و كذلك أخطاء التنبؤ تزداد لكلا النموذجين كلما زاد وقت الأفق. إلى جانب ذلك، خلال الحالة المضطربة، تحسن النسبة المئوية للنموذج الهجين مقارنة بكل من نمودي FCAST-SARIMA و NN-FCAST من ناحية متوسط RMSE والتي تساوي ما بين ١٣,٤٪ و ٢٦,١٪. نماذج التنبؤ تستخدم في التتابع لتزويد تحقيق كامل على المحتوى الكامل للألكترونات لطبقة الأيونوسفير والتي تمت نمذجتها في منطقة باريت راجا الواقعه في ماليزيا.

## TABLE OF CONTENTS

<b>Contents</b>	<b>Page</b>
AUTHOR DECLARATION	i
BIODATA OF AUTHOR	ii
ACKNOWLEDGEMENTS	iii
ABSTRAK	iv
ABSTRACT	v
MULAKHKHASAL-BAHTH	vi
TABLE OF CONTENTS	vii
LIST OF TABLES	viii
LIST OF FIGURES	ix
LIST OF SYMBOLS	x
LIST OF APPENDICES	xi
ABBREVIATION	xii
<b>CHAPTER 1 INTRODUCTION</b>	
1.1 BACKGROUND	1
1.2 RESEARCH ON MALAYSIA IONOSPHERIC TEC	4
1.3 PROBLEMS STATEMENT	9
1.4 RESEARCH OBJECTIVES	12
1.5 RESEARCH SCOPES	13
1.6 RESEARCH CONTRIBUTIONS	14
1.7 THESIS OUTLINE	14

## CHAPTER 2 LITERATURE REVIEW

2.1	INTRODUCTION	17
2.2	EARTH'S IONOSPHERE	17
2.3	IONOSPHERIC VARIATIONS	21
2.4	IONOSPHERIC TOTAL ELECTRON CONTENT (TEC)	23
2.5	ESTIMATION AND FORECASTING IONOSPHERIC TEC MODELS	28
2.5.1	Models for estimating the ionospheric TEC	29
2.5.2	Models for forecasting the ionospheric TEC	33
2.6	NEURAL NETWORK (NN) MODEL IN NON-LINEAR APPROXIMATION	40
2.6.1	Architecture of Neural Network	43
2.6.2	Feed forward with back propagation algorithm	45
2.7	SEASONAL AUTOREGRESSIVE INTEGRATED MOVING AVERAGE (SARIMA) MODEL IN LINEAR APPROXIMATION	51
2.7.1	Autoregressive (AR) processes	51
2.7.2	Moving average (MA) processes	52
2.7.3	Autoregressive moving average (ARMA) processes	53
2.7.4	Autoregressive integrated moving average (ARIMA) processes	53
2.7.5	Seasonal autoregressive integrated moving average (SARIMA) processes	54
2.7.6	SARIMA model development based on Box-Jenkins technique	56
2.8	IONOSPHERIC TEC BASED ON GPS MEASUREMENTS	62
2.8.1	Radio waves refraction in ionosphere	64
2.8.2	Derivation of Total Electron Content from ionospheric refraction	70
2.8.3	Derivation of Total Electron Content from GPS measurements	72
2.9	SUMMARY	77

## CHAPTER 3 METHODOLOGY DEVELOPMENT OF NNS AND HYBRID SARIMA-NN MODELS

3.1	INTRODUCTION	78
3.2	TEC DATA AT WIRELESS AND RADIO SCIENCE CENTRE (WARAS), PARIT RAJA STATION	79
3.2.1	Single Layer Model and mapping function	84
3.3	DATA PROCESSING FOR IONOSPHERIC TEC MODELLING	86
3.4	DEVELOPMENT OF NEURAL NETWORK-BASED TEC ESTIMATION MODEL	88
3.4.1	Determination of optimum input space	91
3.4.1.1	Optimum solar proxies	96
3.4.1.2	Optimum magnetic proxies	104
3.4.2	Determination of optimum hidden neurons	106
3.4.3	Determination of optimum training algorithm	107
3.4.4	Optimum architecture of neural network	118
3.4.5	Verification of NN model	121
3.5	DEVELOPMENT OF HYBRID SARIMA-NEURAL NETWORK-BASED TEC FORECASTING MODEL	122
3.5.1	Modelling of SARIMA	124
3.5.2	Modelling of neural network	139
3.5.3	Optimum Hybrid SARIMA-NN model	144
3.5.4	Single model Techniques	145
3.6	ASSESSMENT OF RESULTS	147
3.7	SUMMARY	149

## CHAPTER 4 RESULTS AND DISCUSSIONS

4.1	INTRODUCTION	151
4.2	RECONSTRUCTION OF MISSING GPS TEC DATA	152
4.2.1	Interpolate and Extrapolate missing data up-to 6-days	152
4.2.2	Interpolate and Extrapolate missing data up-to 30-days	155
4.3	SEASONAL TEC ESTIMATION	158

4.4	DISTURBED DAYS TEC ESTIMATION	163
4.5	FORECASTING GPS TEC	171
4.5.1	Forecasting GPS TEC during quiet condition	172
4.5.2	Forecasting GPS TEC during moderate condition	174
4.5.3	Forecasting GPS TEC during disturbed condition	176
4.6	SUMMARY	180
<b>CHAPTER 5 CONCLUSIONS</b>		
5.1	INTRODUCTION	183
5.1.1	Identification on the space weather parameters that contribute to TEC modelling	183
5.1.2	Development of TEC estimation model based on neural network technique	185
5.1.3	Investigation on the predictability of TEC using NN to estimate seasonal TEC and disturbed days TEC	187
5.1.4	Development of TEC forecasting model based on hybrid SARIMA-NN model	188
5.2	FUTURE WORKS	191
	REFERENCES	193
	APPENDICES	207

## LIST OF TABLES

	<b>Page</b>
Table 2.1 : Summary of regional TEC estimation models	31
Table 2.2 : Summary of regional TEC forecasting models	35
Table 2.3 : The parameters used in (Cander et al.,1998) forecasting model	37
Table 2.4 : Non-seasonal theoretical ARIMA models	59
Table 3.1 : Combinations of solar proxies	103
Table 3.2 : Combinations of magnetic and solar proxies	105
Table 3.3 : Training algorithms used in NN training	108
Table 3.4 : Comparison of performance index between the training algorithms	117
Table 3.5 : SARIMA models with the AIC, Ljung-Box statistic and Chi-square values	135
Table 3.6 : Combinations of residual lag numbers	142
Table 3.7 : Input parameters of the FCAST-NN model	146
Table 4.1 : Average GPS TEC, RMSE, normalized RMSE and relative correction between the GPS TEC and the estimated values; NN2 TEC and IRI TEC during March equinox, June solstice, October equinox and December solstice in 2006 over Parit Raja station	161
Table 4.2 : Average GPS TEC, RMSE, normalized RMSE and relative correction between the GPS TEC and the estimated values; NN2 TEC and IRI TEC during the geomagnetic storm from 14-16 December 2006 over Parit Raja station	167
Table 4.3 : Average GPS TEC, RMSE, normalized RMSE and relative correction between the GPS TEC and the estimated values; NN2 TEC and IRI TEC during the	170

geomagnetic storm from 13-15 April 2006 over Parit Raja station

Table 4.4 : Average GPS TEC, normalized RMSE and relative correction between the GPS TEC and the forecast values; Hybrid TEC, SARIMA TEC and NN TEC during quiet, moderate and disturbed conditions over Parit Raja station 179



## LIST OF FIGURES

		<b>Page</b>
Figure 2.1	: Dominant ion population and ionospheric plasma density with various layers	19
Figure 2.2	: Profiles of plasma density during day and night	20
Figure 2.3	: Ionospheric effects on the radio wave technologies	24
Figure 2.4	: Propagation of radio waves is disrupted by the population of electron in the Earth's ionosphere	25
Figure 2.5	: A general neuronal model with bias	41
Figure 2.6	: A multilayer network with a single hidden layer	45
Figure 2.7	: Box-Jenkins modelling approach	57
Figure 3.1	Process of Extracting Ionospheric TEC data from the GISTM receiver at Parit Raja station, Malaysia	80
Figure 3.2	: Ionospheric Single Layer thin-shell Model (SLM)	85
Figure 3.3	: Flow diagram for TEC modelling using NN and hybrid SARIMA-NN models	87
Figure 3.4	: Flow diagram for development of ionospheric TEC estimation model based on Neural Network technique	90
Figure 3.5	: Proxies are averaged in different smoothing schemes	97
Figure 3.6	: (a) Daily, (b) 27 days and (c) 81 days smoothing backward means for SSN during 2005 and 2006	99
Figure 3.7	: (a) Daily, (b) 27 days and (a) 81 days smoothing centered means for SSN during 2005 and 2006	100
Figure 3.8	: Combinations of different periods for SSN, $F_{10.7}$ and $S_{10.7}$	101
Figure 3.9	: Linear regression between the observed and estimated TEC values using (a) GDA, (b) RP, (c) LM and (d) BFG algorithms	110

Figure 3.10	: Linear regression between the observed and estimated TEC values using (a) CGB, (b) CGF, (c)CGP, and (d) SCG algorithms	111
Figure 3.11	: Computed error values between GPS TEC and NN TEC based on (a) GDA, (b) RP, (c) LM and (d) BFG algorithms	113
Figure 3.12	: Computed error values between GPS TEC and NN TEC based on (a) CGB, (b) CGF, (c) CGP, and (d) SCG algorithms	114
Figure 3.13	: Time line of the training algorithms in seconds	116
Figure 3.14	: Optimal feed forward neural network architecture for TEC estimation model over Parit Raja	119
Figure 3.15	: Scatter plot and correlation coefficient, $R^2$ between the observed TEC and estimated TEC	122
Figure 3.16	: Flow diagram for development of forecasting TEC model based on the hybrid technique	125
Figure 3.17	: Hourly variation of TEC in June 2005 at Parit Raja	127
Figure 3.18	: Autocorrelogram of the TEC time series in June 2005	129
Figure 3.19	: Stationary TEC time series, $z_t$ in June 2005	131
Figure 3.20	: (a) The autocorrelation function, ACF and (b) partial autocorrelation, PACF plots of the stationary TEC time series, $z_t$ for June 2005	133
Figure 3.21	: Autocorrelogram of the residual	138
Figure 4.1	: Comparison between (a) NN1 TEC (interpolation) and (b) NN2 TEC (extrapolation) against the GPS TEC values from 1 - 6 March 2006 over Parit Raja station	153
Figure 4.2	: RMSE and Crel values versus the percentage of missing data, for NN1 (interpolation) and NN2 (extrapolation) model for March 2006 over Parit Raja station	156
Figure 4.3	: Comparison seasonal TEC variations between GPS TEC, NN2 TEC and IRI TEC at Parit Raja station for (a) March (Vernal Equinox), (b) June (Summer Solstice), (c) September (Autumn Equinox), and (d) December (Winter Solstice) in 2006	159

Figure 4.4	:	Dst and the corresponding GPS TEC, NN2 TEC and IRI TEC from 14-16 December 2006 over Parit Raja station	166
Figure 4.5	:	Dst and the corresponding GPS TEC, NN2 TEC and IRI TEC from 13-15 April 2006 over Parit Raja station	169
Figure 4.6	:	Comparison between GPS TEC and the hourly forecast TEC values produced by (a) hybrid SARIMA-NN model, (b) FCAST-SARIMA model, (c) FCAST-NN model during quiet days (10 - 12 October 2006) over Parit Raja	173
Figure 4.7	:	Comparison between GPS TEC and the hourly forecast TEC values produced by (a) hybrid SARIMA-NN model, (b) FCAST-SARIMA model, (c) FCAST-NN model during moderate days (9 - 11 November 2006) over Parit Raja	175
Figure 4.8	:	Comparison between GPS TEC and the hourly forecast TEC values produced by (a) hybrid SARIMA-NN model, (b) FCAST-SARIMA model, (c) FCAST-NN model during disturbed days (14 -16 December 2006) over Parit Raja	178
Figure 4.9	:	RMSE values for Hybrid, SARIMA and NN models during the quiet, moderate and disturbed conditions in 2006 over Parit Raja	180

## LIST OF SYMBOLS

$B$	:	backward shift operator
$p$	:	order of non-seasonal autoregressive
$q$	:	order of non-seasonal moving average
$d$	:	order of differencing non-seasonal component
$P$	:	order of seasonal autoregressive
$Q$	:	Order of seasonal moving average
$D$	:	order of differencing seasonal component
$s$	:	length of seasonal period
$\Phi$	:	coefficient of seasonal autoregressive
$\Theta$	:	coefficient of seasonal moving average
$\phi$	:	coefficient of non-seasonal autoregressive
$\theta$	:	coefficient of non-seasonal moving average
$a_t$	:	random errors
$n_\phi$	:	phase refractive index
$n_g$	:	group refractive index
$v_\phi$	:	phase velocity
$v_g$	:	group velocity
$\frac{dn_\phi}{df}$	:	change of phase refractive index with respect to the frequency.
$\omega_N$	:	angular plasma frequency
$\omega_B$	:	electron gyrofrequency

$\omega$	:	angular frequency of the propagating wave,
$\omega_L$	:	longitudinal component of the electron gyrofrequency,
$\omega_T$	:	transverse component of the electron gyrofrequency,
$\nu$	:	angular collision frequency between electrons and heavier particles
$\theta$	:	angle between the geomagnetic field vector and the propagation wave direction.
$N$	:	electron density
$e$	:	electron charge
$\epsilon_0$	:	electric permittivity of free space
$\Delta I_{P_1}$	:	pseudo-range ionospheric induced errors (m) at L1 frequency
$\Delta I_{P_2}$	:	pseudo-range ionospheric induced error (m) at L2 frequency
$\Delta I_{\phi_1}$	:	carrier ionospheric induced errors (m) at L1 frequency
$\Delta I_{\phi_2}$	:	carrier ionospheric induced errors (m) at L2 frequency
$\lambda_1$	:	wavelength of the signal (m) at L1 frequency
$\lambda_2$	:	wavelength of the signal (m) at L2 frequency
$N_1$	:	carrier phase integer ambiguities between satellite and receiver (cycle) at L1 frequency
$N_2$	:	carrier phase integer ambiguities between satellite and receiver (cycle) at L2 frequency
$bS_{P_1}$	:	pseudo-range satellite hardware delays (m) at L1 frequency
$bS_{P_2}$	:	pseudo-range satellite hardware delays (m) at L2 frequency
$bS_{\phi_1}$	:	carrier phase satellite hardware delays (m) at L1 frequency
$bS_{\phi_2}$	:	carrier phase satellite hardware delays (m) at L2 frequency

- $bR_{P_1}$  : pseudo-range GPS receiver hardware delays (m) at L1 frequency  
 $bR_{P_2}$  : pseudo-range GPS receiver hardware delays (m) at L2 frequency  
 $bR_{\Phi_1}$  : carrier phase GPS receiver hardware delays (m) at L1 frequency  
 $bR_{\Phi_2}$  : carrier phase GPS receiver hardware delays (m) at L2 frequency  
 $\Delta_{multipath,P_1}$  : pseudo-range multipath effects (m),  
 $\Delta_{multipath,P_2}$   
 $\Delta_{multipath,\Phi_1}$  : carrier phase multipath effects (m),  
 $\Delta_{multipath,\Phi_2}$   
 $\varepsilon(P_1), \varepsilon(P_2)$  : pseudo-range measurement noises (m),  
 $\varepsilon(\Phi_1), \varepsilon(\Phi_2)$  : carrier phase measurement noises (m).

## LIST OF APPENDICES

	Page
APPENDIX A : ESTIMATED AND SMOOTHED RECEIVER BIAS	207
APPENDIX B : SMOOTHING AVERAGE OVER $F_{10.7}$ AND $S_{10.7}$ PROXIES	209
APPENDIX C : GEOMAGNETIC STORMS DURING FEBRUARY 2005 TO 2006 WITH THE CORRESPONDING GPS TEC AND MEDIAN TEC VALUES	213

## ABBREVIATION

ACF	Autocorrelation Function
AIC	Akaike Information Criterion
ap	Equivalent three hourly planetary amplitude
AR	Autoregressive
ARIMA	Autoregressive Integrated Moving Average
ARMA	Autoregressive Moving Average
BFG	Boyden, Fletcher, Goldfarb and Shanno update
CGB	Powell – Beale restarts conjugate gradient
CGF	Fletcher – Reeves Update conjugate gradient
CGP	Polak-Ribiere Update conjugate gradient
CME	Coronal Mass Ejections
Crel	Relative correction
DN	Day Number
Dst	Disturbance Storm Time
Eabs	Absolute error
EIA	Equatorial Ionization Anomaly
Erel	Relative error
EUV	Extreme Ultra-violet
F <sub>10.7</sub>	Solar Radio Flux
FCAST-NN	Forecast NN
FCAST-SARIMA	Forecast SARIMA
GAGAN	GPS Aided GEO Augmented Navigation
GDA	Batch gradient descent with variable learning rate
GISTM	GPS Ionospheric Scintillation and TEC Monitor
GNSS	Global Navigation Satellite Systems
GPS	Global Positioning System
HF	High Frequency
HR	Hour
HYBRID SARIMA-NN	Hybrid Seasonal Autoregressive Integrated Moving Average-Neural Network
IGS	International GNSS Service
IPP	Ionospheric Pierce Point
IRI	International Reference Ionosphere
ISIS	International Satellites for Ionospheric Studies
JUPEM	Jabatan Ukur dan Pemetaan Malaysia
LM	Levenberg-Marquardt algorithm
LT/UT	Local or Universal Time
MA	Moving Average
MASS	Malaysia Active GPS System
MLE	Maximum Likelihood Estimation
MSE	Mean Square Error

M-SLM	Modify Single Layer Model
MyRTKnet	Malaysia RTK Network
NGDC	National Geophysical Data Centre
NN	Neural Network
PACF	Partial Autocorrelation Function
PPP	Precise Point Positioning
PPS	Precise Positioning Service
PRE	Pre-Reversal Enhancement
RACF	Residual Autocorrelation Function
RINEX	Receiver Independent Exchange Format
RMSE	Root Mean Square Error
ROT	Rate of TEC
RP	Resilient back-propagation algorithm
RTK	Real Time Kinematic
$S_{10.7}$	Solar extreme ultraviolet (EUV) flux
SA	Selectivity Availability
SARIMA	Seasonal Auto Regressive Integrated Moving Average
SC	Solar Cycle
SCG	Scaled conjugate gradient
SEM	Solar EUV Monitor
SLM	Single Layer Model
SOHO	Solar And Heliospheric Observatory
SPS	Standard Positioning Service
SSE	Sum of Squared Errors
SSN	Sunspot Number
sTEC	Slant TEC
TEC	Total Electron Content
TECU	Total Electron Content Unit
URSI	International Union on Radio Science
USDoD	United States Department of Defense
VHF	Very High Frequency
VRS	Virtual Reference Station
vTEC	Vertical TEC
WARAS	Wireless and Radio Science Centre
WDC	World Data Centre